Proc. Indian Acad. Sci. (Earth Planet. Sci.), Vol. 104, No. 3, September 1995, pp. 385–405.

Structural and textural development in Singhbhum shear zone, eastern India

DHRUBA MUKHOPADHYAY[a] and GAUTAM KUMAR DEB[b]

[a]Department of Geology, University of Calcutta, 35, Ballygunge Circular Road, Calcutta 700019, India

[b]Geological Studies Unit, Indian Statistical Institute, Calcutta 700035, India

Abstract. The rocks within the Singhbhum shear zone in the North Singhbhum fold belt, eastern India, form a tectonic melange comprising granitic mylonite, quartz-mica phyllonite, quartz-tourmaline rock and deformed volcanic and volcaniclastic rocks. The granitic rocks show a textural gradation from the least-deformed variety having coarse- to medium-grained granitoid texture through augen-bearing protomylonite and mylonite to ultramylonite. Both type I and type II S-C mylonites are present. The most intensely deformed varieties include ultramylonite. The phyllosilicate-bearing supracrustal rocks are converted to phyllonites. The different minerals exhibit a variety of crystal plastic deformation features. Generation of successive sets of mylonitic foliation, folding of the earlier sets and their truncation by the later ones results from the progressive shearing movement. The shear sense indicators suggest a thrust-type deformation. The microstructural and textural evolution of the rocks took place in an environment of relatively low temperature, dislocation creep accompanied by dynamic recovery and dynamic recrystallization being the principal deformation mechanisms. Palaeostress estimation suggests a flow stress within the range of 50–190 MPa during mylonitization.

Keywords. Singhbhum shear zone; mylonites; texture; shear sense indicators.

1. Introduction

Within the Proterozoic fold belt of North Singhbhum in eastern India, a prominent shear zone is developed close to its southern contact with the Archaean craton of Singhbhum Granite. The Singhbhum shear zone marks the junction between the overlying Chaibasa Formation and the underlying Dhanjori Group (Dunn and Dey 1942; Sarkar and Saha 1962). The Chaibasa Formation is predominantly made up of pelitic schists with a few thin but persistent bands of quartzite. The Dhanjori Group comprises a conglomerate-arkose-phyllite assemblage associated with mafic to ultramafic metavolcanic rocks. The Singhbhum shear zone is an arcuate ductile shear zone (Ghosh and Sengupta 1987, 1990) whose trend changes from E-W in the western part to NNE-SSW in the eastern part. It is a high strain zone that dips northerly and is clearly demarcated by a number of lenticular bodies of granite mylonite. The present study is confined to the south-eastern sector of the shear zone (figure 1), extending from Surda (22° 33′ 30″ N: 86° 26′ 35″ E) to Kanyaluka (22° 28′ 30″ N: 86° 31′ 00″ E). Here the width of the shear zone is about 850 m in the central part, which decreases towards northwest and southeast. Granite mylonite bands are associated with bands of deformed metasedimentary and metabasic rocks belonging to both the Chaibasa Formation and the Dhanjori Group, and the total assemblage forms a sort of tectonic melange. The boundaries of the shear zone with the Chaibasa Formation to the northeast and the Dhanjori Group to the southwest are not sharp. Pelitic schists with discontinuous horizons of phyllonitic mica schist (Chaibasa Formation) occur to the northeast of the shear zone; to the southwest metabasic rocks with bands of cross-bedded quartzite (Dhanjori Group) are present. The mylonitized granite bodies within the shear zone are interpreted to have intruded the supracrustal rocks at an early stage of the deformation history (Dasgupta *et al* 1993).

The geometry of the folds and their sequence of development are similar in the rocks within and outside the shear zone. The mylonitic foliation within the shear zone is subparallel to the axial plane schistosity of the dominant fold set outside the shear zone (Naha 1965; Mukhopadhyay *et al* 1975; Ghosh and Sengupta 1987, 1990). Within the granites of the shear zone there is a wide range of textural gradation, from the least-deformed variety with coarse- to medium-grained granitoid texture through augen-bearing protomylonite and mylonite (Berthé *et al* 1979) to feldspathic schists free from visible augen (ultramylonite). The mineralogical composition of rocks within the shear zone indicates low grade (chlorite-biotite zone) metamorphic condition during deformation. This work describes the textural and structural evolution of the mylonites within the shear zone.

2. Lithological types

The coarser grained granitoid rocks range in composition from tonalite to granite (Dasgupta *et al* 1993). Where mildly deformed they contain lenticular porphyroclasts (augen) of plagioclase, or plagioclase + quartz, and rarely of microcline + quartz or quartz alone.

More intense deformation has changed the granitic rocks into feldspathic schists some of which are banded and contain a few mm thick biotite-rich layers alternating with a few mm to about 5 cm thick quartzofeldspathic layers. In the non-banded feldspathic schist thin streaks of biotite with or without chlorite define a foliation. Dynamically recrystallized fine-grained groundmass constitutes more than 80% of the rock, and the remaining part is made up of porphyroclasts of plagioclase and coarse grains and knots of mafic minerals. These rocks may be designated as ultramylonite (White 1976; Berthé *et al* 1979).

At places 1–5 cm thick bands and stringers of medium-grained aplite showing pinch and swell structure are aligned parallel to the foliation in quartzofeldspathic ultramylonite (figure 2). These possibly represent the protoliths from which the non-banded feldspathic schist was derived.

Phyllonitic mica schist occurs in the upper (northern) levels of the shear zone; in the central part 2–3 m thick bands of phyllonite alternate with mylonitized granite.

The other important rock type within the shear zone is quartz-chlorite schist which is a fine-grained granular rock with alternate quartz-rich and chlorite-rich layers. This rock possibly represents original volcaniclastic sediments. Dark ellipsoidal fragments of metamorphosed amygdaloidal mafic rock and elongate clots of recrystallized quartz (? deformed amygdules) are important constituents of the rock. Both the fragments and the quartz clots have their long dimension aligned down the dip of the schistosity. At places the rock grades into chlorite schist and chlorite-bearing quartzite.

A number of lenses of apatite- and magnetite-bearing schist extend parallel to the regional foliation. Tourmalinite occurs as a thin band underlying the feldspathic schist

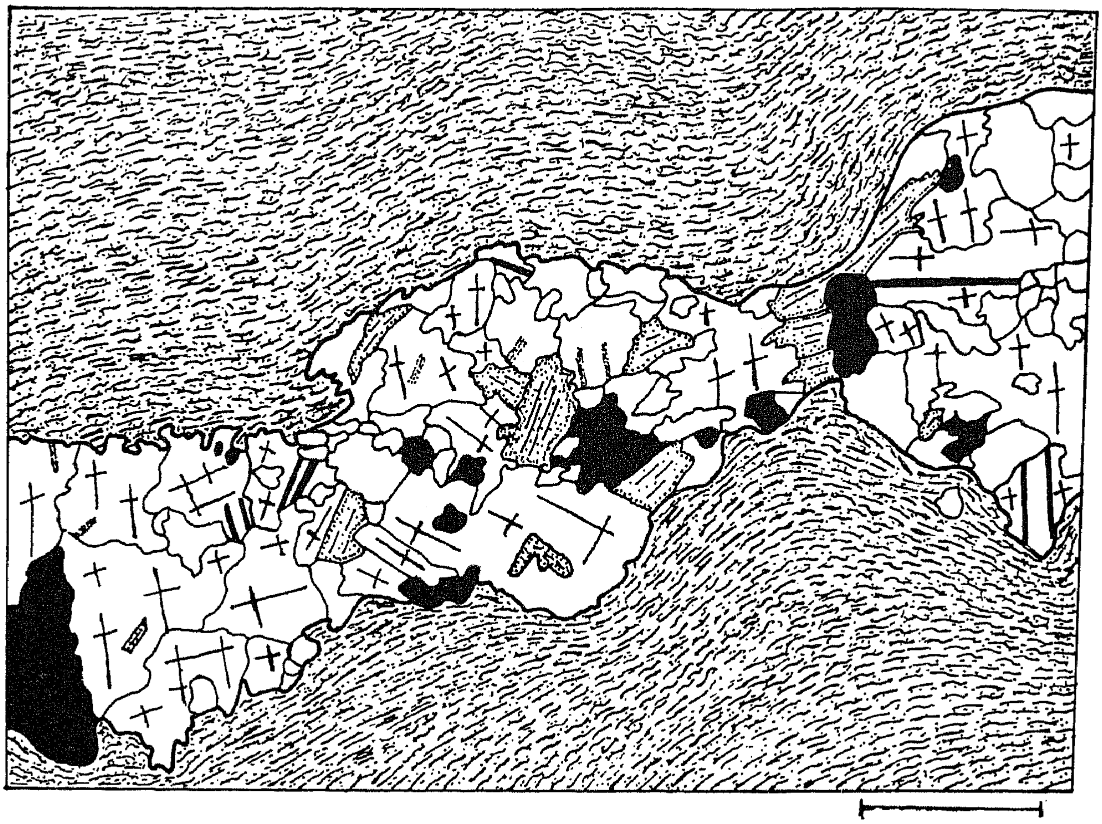

Figure 2. Sketch drawn from thin section showing pinch and swell structure in aplite within mylonite, scale bar – 0·5 mm.

and also as flattened lenses (Deb and Mukhopadhyay 1991). Small discontinuous bands of banded quartz-magnetite rock occur in the upper part of the shear zone. A few lenses of quartzite of the Dhanjori Group are present in the southwestern part of the shear zone.

3. Megascopic structural features within the shear zone

3.1 *Bedding*

Bedding is recognizable in the tourmalinite, in the banded magnetite quartzite and also in the Dhanjori quartzite.

3.2 *Mylonitic banding* (S_b) *and mylonitic foliation* (S_m)

In the banded feldspathic schist, whose protolith was probably a banded migmatite, the mylonitic banding (S_b) is defined by regular alternation of quartz-feldspar-rich and biotite-rich layers (2–50 mm thick). The mylonitic banding is involved in nearly isoclinal intrafolial folding and the folds are often of reclined geometry.

In the augen gneiss lenticular feldspathic and quartzose augen are wrapped around by thin micaceous laminae representing the mylonitic foliation (S_m). In the feldspathic schist thin films of mica with anastomosing pattern wrap round the relict porphyroclasts of quartz and feldspar (figure 3a). Preferred alignment of chlorite and elongate grains of quartz define the mylonitic foliation in the deformed volcanic and volcaniclastic rocks.

In many of the rocks in the shear zone only one orientation of mylonitic foliation is megascopically recognizable, although under the microscope S- and C-planes making small angles with each other are identifiable. The composite mylonitic foliation observed

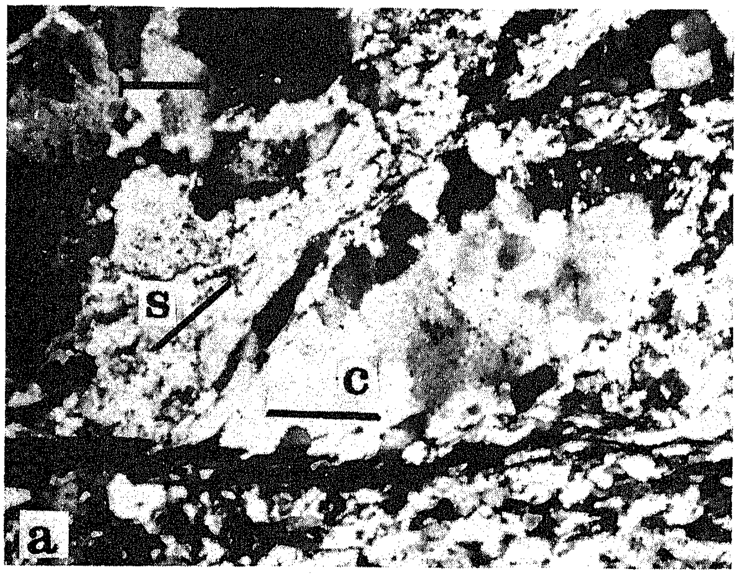

Figure 3(a). Micaceous laminae curving around quartzose porphyroclast defining S-C fabric in augen gneiss, scale bar – 0·2 mm.

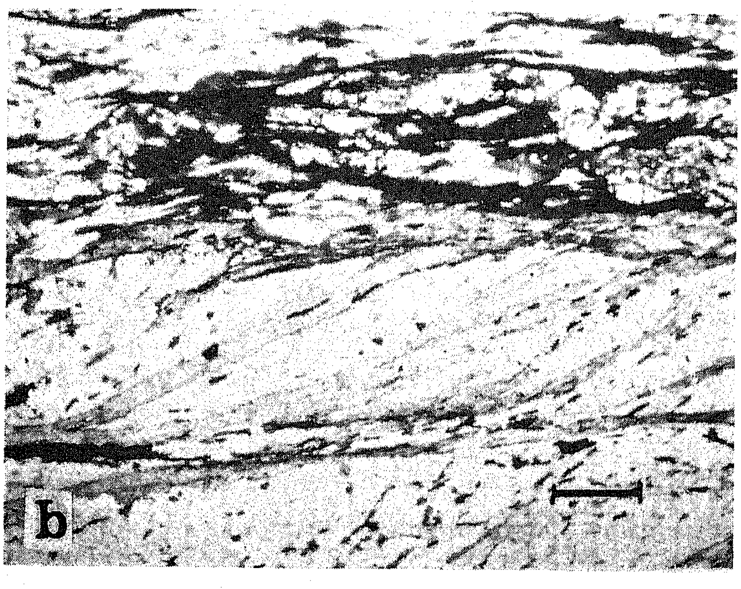

Figure 3(b). An earlier mylonitic foliation cut across by later micaceous laminae. The earlier foliation shows sigmoidal curvature indicating sense of movement on the later plane, scale bar – 0·5 mm.

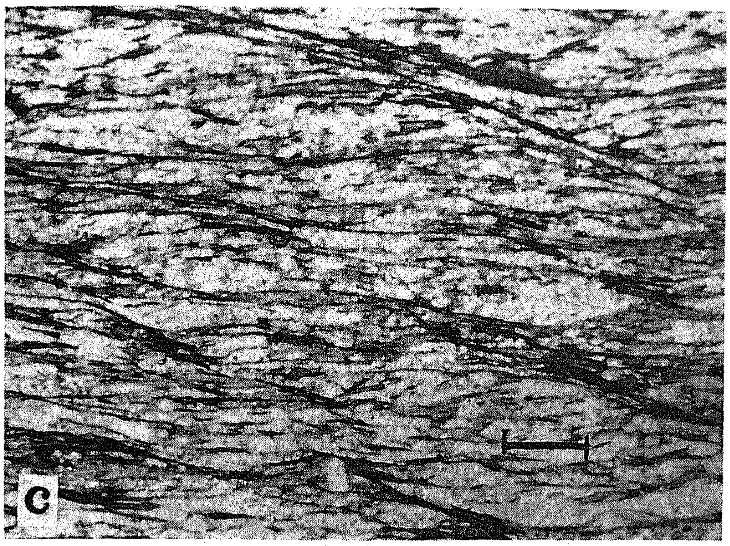

Figure 3(c). Shear bands (*C'*) causing sigmoidal curvature to the earlier planes, scale bar – 0·5 mm.

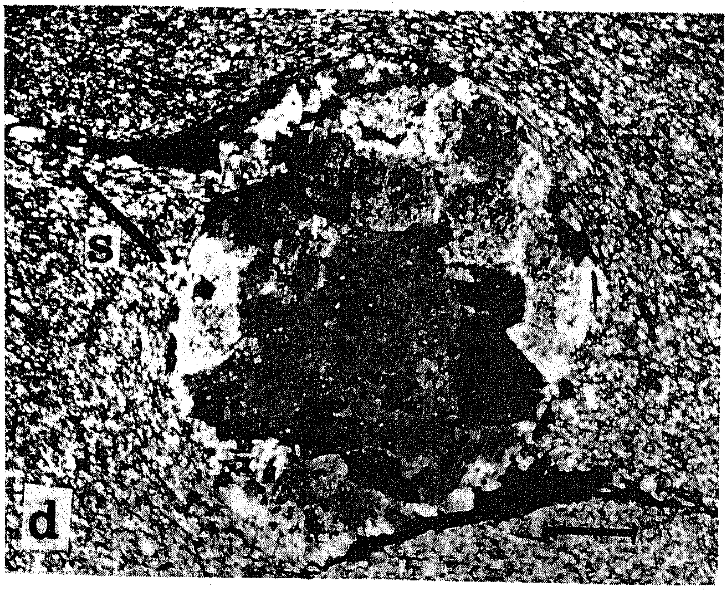

Figure 3(d). Round quartz-plagioclase porphyroclast in an ultramylonitic matrix; note asymmetrical deflection of biotitic lamina, *s*-mylonitic foliation, scale bar – 0·5 mm.

in outcrops dips northerly at 40°–60°. Some of the feldspathic schists display sequential development of sets of mylonitic foliation (figures 3b, 4a, 4b, 4c). The earliest set is often folded into tight to isoclinal intrafolial folds, and these are cut across by a second set of mylonitic foliation. At places the second set itself is folded into broad warps and is cut across by a still later set of movement planes (figure 4b). However, these successive sets of mylonitic foliation are now at small angles to one another and could not be measured separately in the field.

A schistosity defined by preferred arrangement of flakes of mica and chlorite and elongate grains of quartz has developed parallel to the axial planes of reclined folds which are defined by quartz veins and by mylonitic banding. On the hinges of the folds

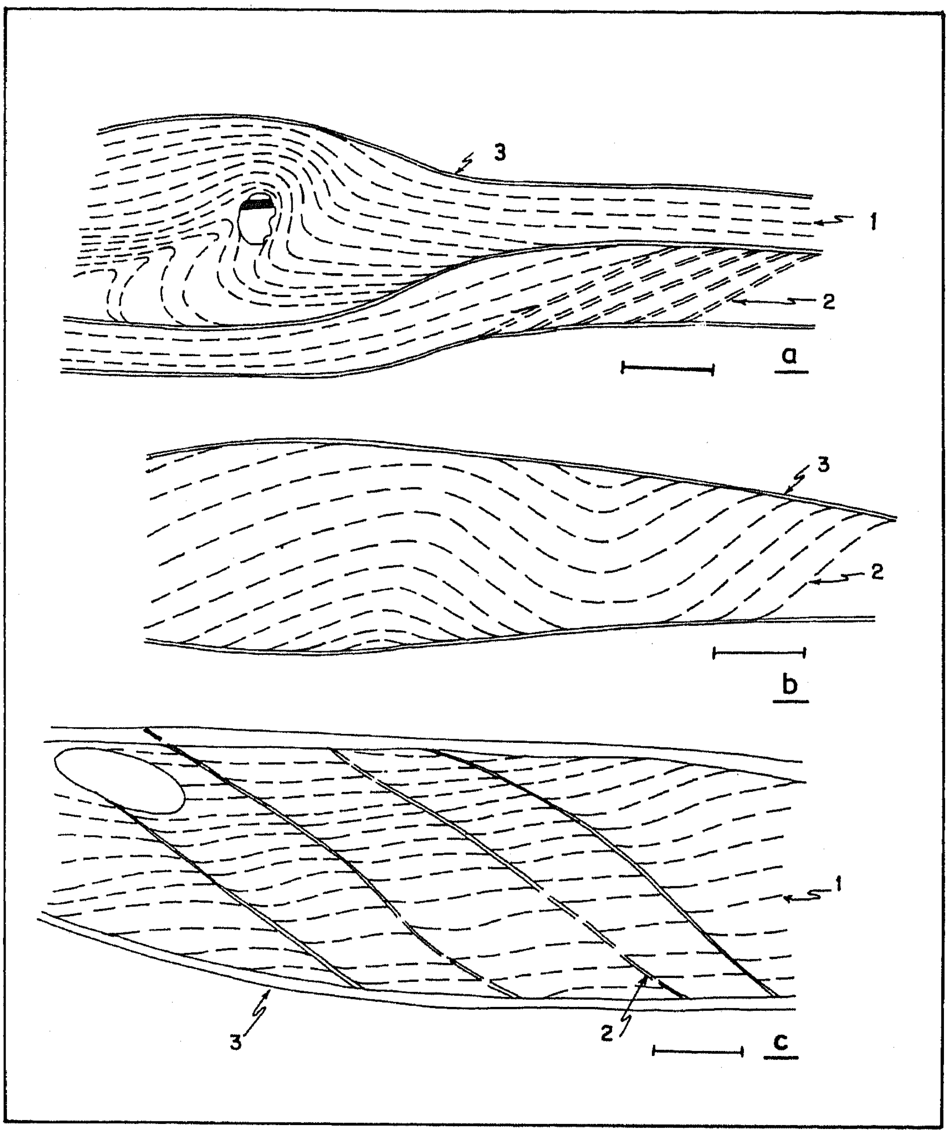

Figure 4. (**a**) Sketch drawn from thin section showing relation between different generations of mylonitic foliation, **1** – earliest foliation, **3** – last foliation, scale bar – 1 mm; (**b**) Sketch drawn from thin section showing broad warps on second generation mylonitic foliation (2) truncated by later movement planes (3), scale bar – 0·2 mm; (**c**) Features same as in figure 4a, scale bar – 0·5 mm.

the schistosity makes an angle with the mylonitic foliation. Under the microscope it is apparent that this schistosity has also acted as movement planes.

3.3 *Later shear bands or C′-planes*

A later set of shear bands or C′-planes (Simpson 1984), represented by thin micaceous laminae, cuts across the mylonitic foliation and gives rise to sigmoidal curvature of the latter. The shear bands have nearly the same strike as the mylonitic foliation but they dip more gently. There is always an up-dip sense of movement of the overlying block on such planes. The nature of deflection of the main foliation by the shear bands (figure 3c) makes the latter comparable to extensional crenulation cleavage (Platt 1979; Platt and

Vissers 1980). Though rare, two sets of shear planes analogous to conjugate Riedel shears are seen in some banded mylonites. The sense of movement on these secondary shears indicates up-dip movement of the overlying block in the main shear zone.

3.4 *Crenulation cleavage*

Zonal as well as discrete types of crenulation cleavage (Gray 1977) are developed parallel to the axial planes of later folds which invariably have a sinistral shape in cross section, viewed from the south or southeast. In the phyllonitic mica schist alternate quartzose and phyllosilicate-rich bands have developed parallel to the crenulation cleavage as a result of metamorphic differentiation. Such secondary banding is typically found where the crenulations are asymmetric and the domains in which earlier schistosity makes a high angle with the crenulation cleavage are quartz rich and those in which the angle is low are depleted in quartz. Occasionally these cleavage planes appear as movement planes which cut across sigmoidally curved earlier schistosity planes.

3.5 *Down-dip stretching lineation*

A strong down-dip mineral lineation defined by mica streaks, amphibole needles, and elongate clots of quartz and feldspar is ubiquitously developed on the mylonitic foliation. The axes of reclined folds, rods produced by boudinaging of folded quartz veins, and alternate ridges and grooves on the surface of the quartz rods are parallel to this lineation. In the banded mylonite a down-dip lineation is formed by elongation of mica and quartz streaks. The porphyroblastic knots of tourmaline, biotite and chlorite in the feldspathic schists and the rock fragments in the quartz-chlorite schist are elongated parallel to the down-dip lineation. This linear structure thus represents the direction of maximum elongation on the mylonitic foliation.

3.6 *Minor folds*

A complex pattern of minor folds with diverse styles and orientations are observed within the shear zone (figure 5A). The earliest generation of minor folds recognized in the shear zone is represented by tight to isoclinal folds on the mylonitic banding, which have reclined geometry and have axes parallel to the down-dip stretching lineation. The intrafolial folds developed in the feldspathic schists and the early folds in concordant quartz veins also have reclined geometry.

The later folds in the mylonites vary both in style and orientation. They have the geometry of similar folds with an angular hinge, or of nearly parallel folds with a rounded hinge. They have a consistently sinistral sense of asymmetry in sections viewed from the south or southeast, indicating up-dip movement of the overlying block. The axial planes have nearly the same strike as the mylonitic foliation; they generally have a steeper dip, but with increasing tightness of the folds and increasing axial plunge the amount of dip becomes less and the axial planes become subparallel to the mylonitic foliation.

It is postulated that minor folds were initiated in the shear zone due to perturbations in the flow regime. To start with they had subhorizontal axes at high angles to the

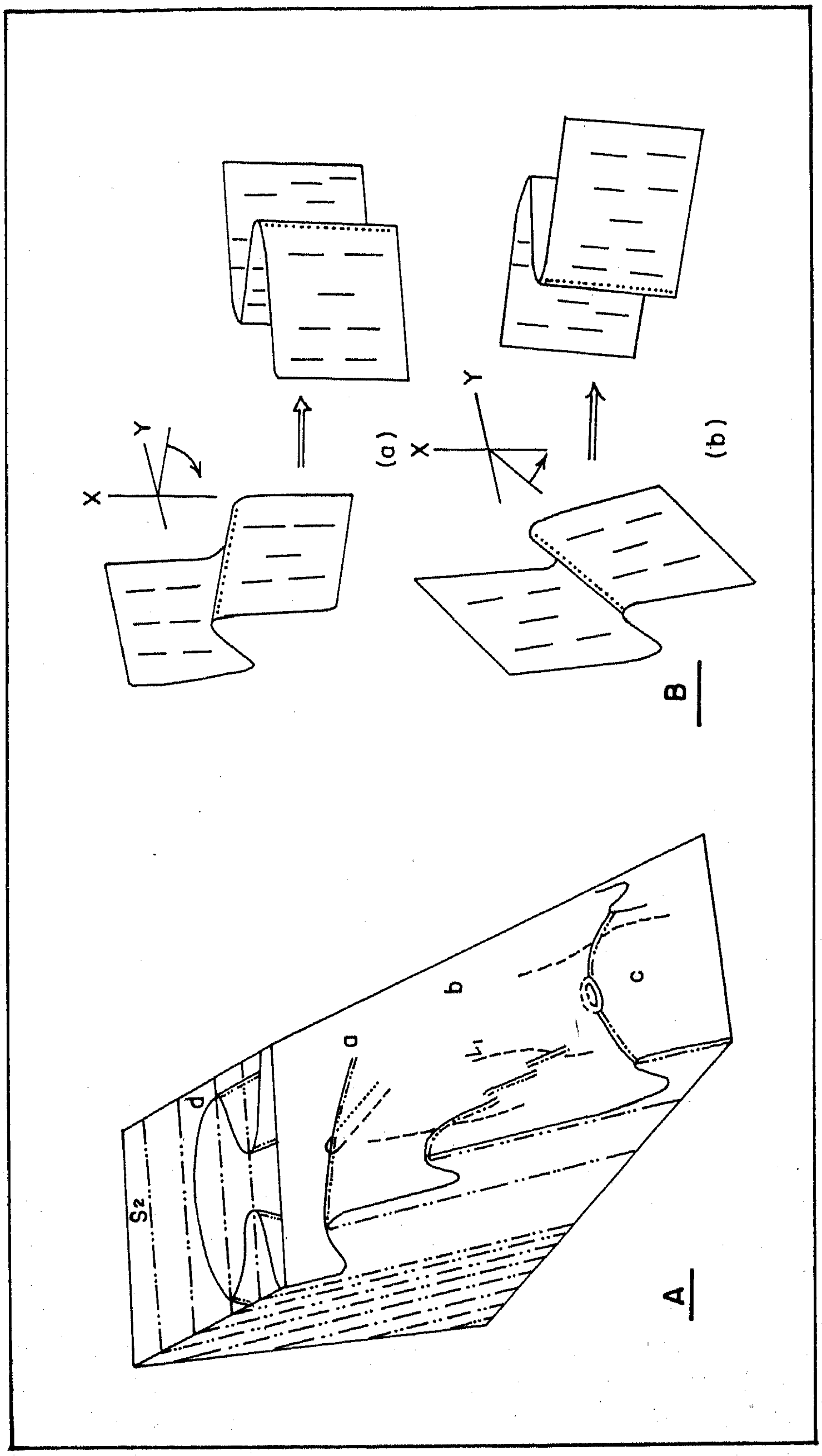

Figure 5. (**A**) Schematic diagram illustrating geometric variation shown by the sinistral folds within the shear zone: (**a**) gently plunging axis, (**b**) steeply plunging axis with en echelon arrangement, (**c**) axis showing gentle culmination, (**d**) sheath fold with steeply plunging axis; (**B**) Schematic diagram illustrating S- and Z-shaped profiles of reclined folds, which result from rotation of axis in clockwise (**a**) and anticlockwise (**b**) senses.

down-dip lineation. The thrust type of movement in the shear zone is responsible for the observed asymmetry of the folds. With progressive deformation the folds became tighter and their axes assumed a steeper plunge as a result of rotation towards the movement direction. In the same process their axial planes rotated towards parallelism with the flow plane. The fold axis was initially subperpendicular to the down-dip lineation. This angle became progressively smaller and finally the two became parallel. Where the lineation and the fold axis are oblique the former goes around the fold hinges. Ghosh and Sengupta (1987) have suggested that the folds in the Singhbhum shear zone were generated by buckling and have evolved, in response to progressive shearing movement, from an initial orientation with axes broadly parallel to the *Y*-axis (subhorizontal) of bulk strain to the final reclined geometry with axes parallel to the northeasterly plunging down-dip lineation (X-axis of bulk strain). We have observed that although the gently or moderately plunging folds are always sinistral in vertical sections viewed from the south or southeast, reclined folds have either S- or Z-shape on horizontal or profile sections. As has already been mentioned, the initial asymmetry of the folds was produced by thrust-type movement in the shear zone. If the axes of initial folds were inclined on either side of the movement direction they would rotate in opposite senses and when they came to attain a reclined geometry their sense of asymmetry on the horizontal surface would be different. Thus a fold initially sinistral in cross section viewed from the south or southeast and with gentle northeasterly plunge, after rotation to a reclined position would show a sinistral shape on a horizontal surface. If it had a gentle southeasterly plunge, after rotation to a reclined position it would show a dextral shape on a horizontal surface (figure 5B). Occasionally individual folds show acute curvature of the axis giving rise to a sheath-like geometry (cf. Cobbold and Quinquis 1980). These folds result from accentuation of slight initial curvature of the fold axis during progressive simple shear deformation.

A set of warps with axial planes transverse to the strike of the mylonitic foliation and axes parallel to the down-dip lineation is ubiquitously developed. This has caused a variation in strike of the main planar fabric within the shear zone. Such folds are due to longitudinal compression and are unrelated to the shear movement.

4. Microstructural and textural features

The rocks of the shear zone, particularly the granites, record a gradual modification of texture in response to increase in the intensity of deformation. Where the intensity of deformation is moderate, S- and C-planes (Berthé *et al* 1979) give rise to rhombic or lenticular domains (figures 3a, 6a) and resultant augen structure in the augen gneiss. Coarse-grained granitic rocks are converted to foliated mylonite with apparently anastomosing foliation planes. With increasing deformation the size and the proportion of the augen diminish. The feldspathic schists are ultramylonites, which rarely preserve relicts of the original rock in the form of thin aplite bands with pinch and swell structure (figure 2) or as isolated lenticular quartz-feldspar porphyroclasts (figure 3d). Preferred dimensional arrangement of tiny elongate grains of quartz and plagioclase defines the mylonitic foliation in the ultramylonite groundmass (figure 7a). The mylonitic foliation curves in harmony with the pinch and swell structure of the aplitic bands; it is also deflected around the isolated porphyroclasts. In some places the ultramylonite bands penetrate into the aplite to separate quartz-feldspar porphyroclasts from the main band (figure 7b).

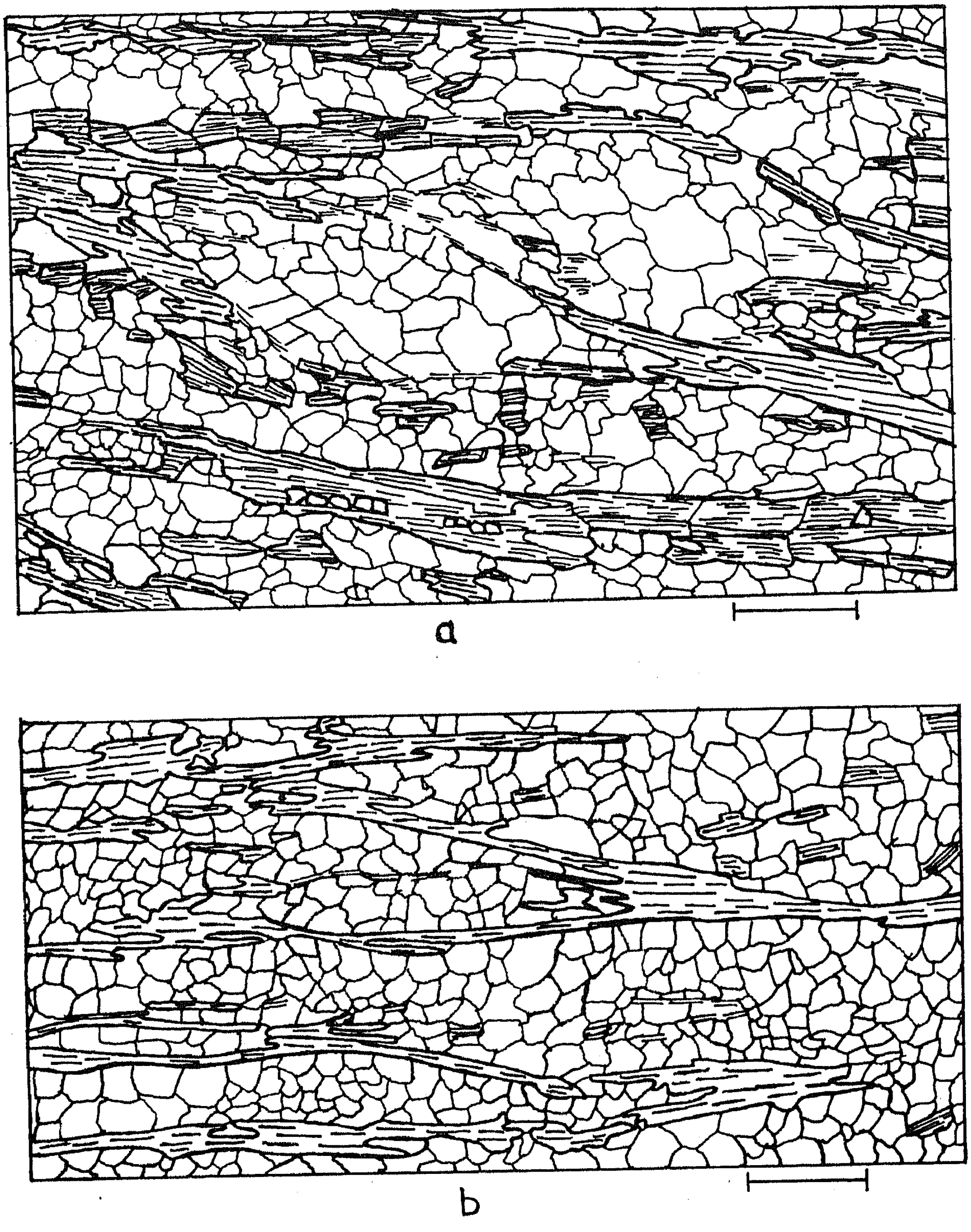

Figure 6. (**a**) Type I S-C mylonite, scale bar – 0·5 mm; (**b**) Type I S-C mylonite showing low angle between S- and C-planes, scale bar – 0·5 mm.

4.1 *Development of S- and C-planes*

In the least-deformed variety of granite a crude mylonitic foliation, defined by recrystallized elongate quartz and feldspar grains (figure 8a), is developed in some wavy planar zones. Occasional chloritic laminae oblique to the mylonitic foliation represent movement planes (C-planes).

In the augen gneiss and protomylonite the dominant foliation is represented by micaceous laminae, which are anastomosing in nature and wrap round the porphyroclasts made up of feldspar, aggregates of quartz and feldspar or rarely only quartz. The fine-grained and shredded mica flakes along these anastomosing laminae indicate that the micaceous laminae acted as movement planes (C-planes). Another set of micaceous laminae which are made up of thin flakes make an acute angle with the C-planes. These two sets of planes delimit lenticular to rhombic fabric domains (figures 3a, 6a) and are interpreted to represent S-C planes (Berthé *et al* 1979; White *et al* 1980). Such rocks are similar to type I S-C mylonites of Lister and Snoke (1984). The angle between S- and C-planes changes from 30°–40° in the less deformed mylonites to 10°–15° in the more deformed ones (figure 6b), implying progressive rotation of the S-planes towards C-planes (cf. Berthé *et al* 1979). The proportion and size of the porphyroclasts are

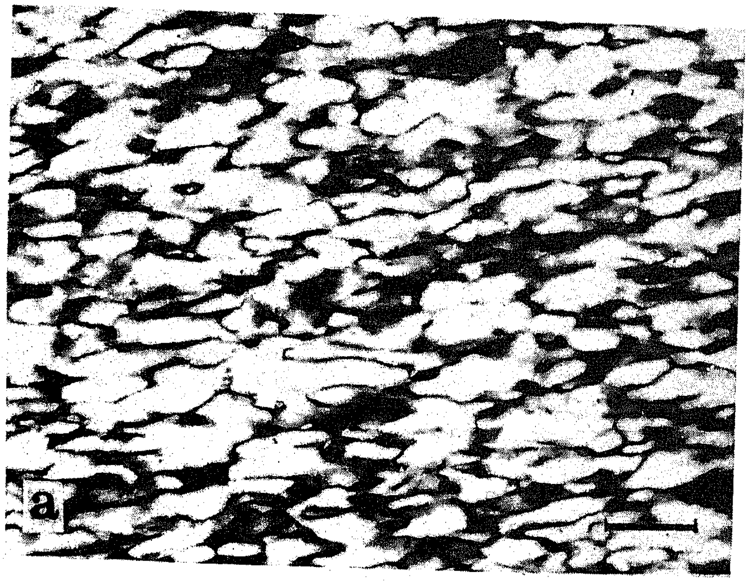

Figure 7(a). Elongate grains of quartz and plagioclase defining mylonitic foliation in ultramylonite, scale bar – 0·05 mm.

Figure 7(b). Ultramylonite tongue penetrating into aplite band separates quartz-feldspar porphyroclasts, scale bar – 0·5 mm.

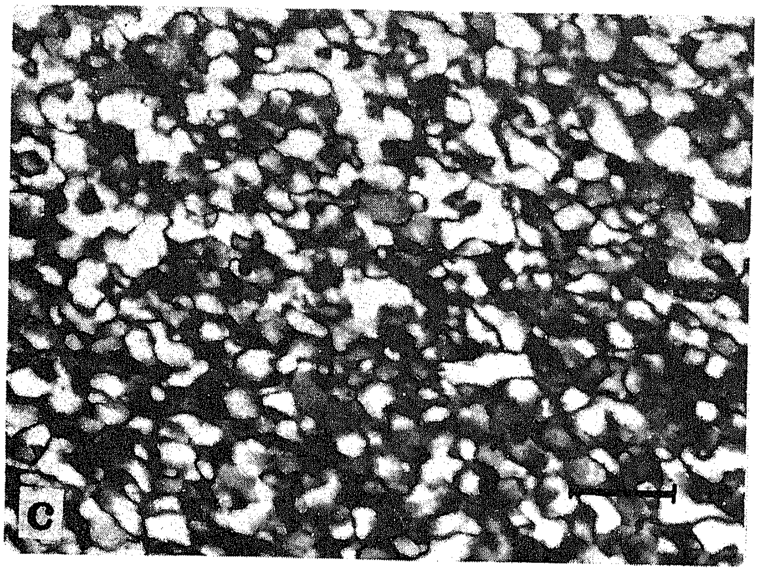

Figure 7(c). Groundmass of ultramylonite showing mosaic of recrystallized polygonal grains, scale bar – 0·05 mm.

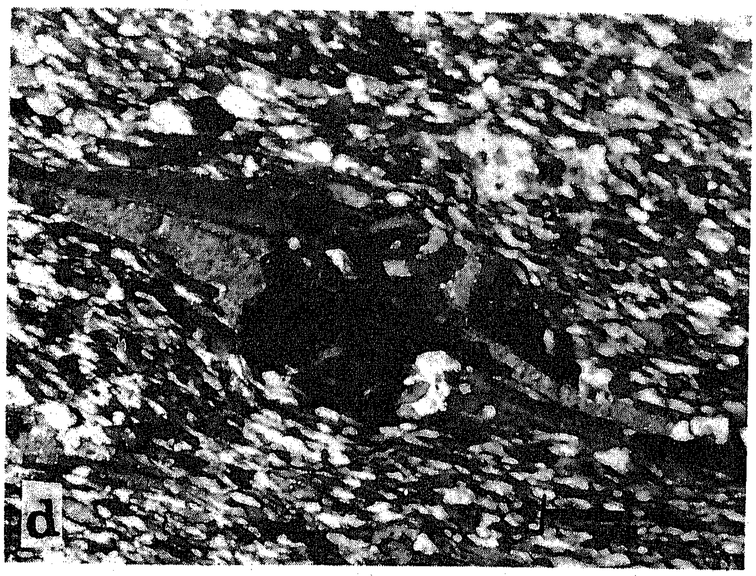

Figure 7(d). σ-type structure defined by pressure fringes made up of chlorite flakes at the edges of tourmaline-quartz knot, scale bar – 0·2 mm.

reduced and consequently the proportion of the finer-grained groundmass also increases (table 1).

In some mylonites, e.g. near Kanyaluka, flat lenses of fine-grained recrystallized quartz or quartz and feldspar and thin streaks or laminae of micaceous material alternate with each other giving rise to a fine mylonitic banding. The elongate quartz ribbons in some rocks are made up of sub-grains or grains with dentate margins. The elongation of the latter defines a planar fabric (S-plane) oblique to the main mica foliation (C-plane; figure 8b) and it records the last incremental strain during shearing deformation (Simpson and Schmid 1983). The texture is similar to the type II S-C mylonites of Lister and Snoke (1984). Within the feldspathic schist the fine-grained matrix shows type I S-C fabric, the angle between S- and C-planes varying from 0° to 40°. Porphyroclasts are either absent or are very sparse. Some samples contain extremely fine-grained ($< 10\ \mu m$) quartzofeldspathic material (figures 3d, 7a, 7c), occasionally containing coarser-grained recrystallized patches and bands. In these rocks the ultramylonitic material is made up of either a mosaic of recrystallized but strained polygonal grains (figure 7c) often meeting at triple junction or very small elongated grains defining a mylonitic foliation (figure 7a). As mentioned earlier the feldspathic schists record the generation of successive sets of C-planes and transposition of the earlier mylonitic foliation. The hinges of folds on mylonitic foliation often become sites

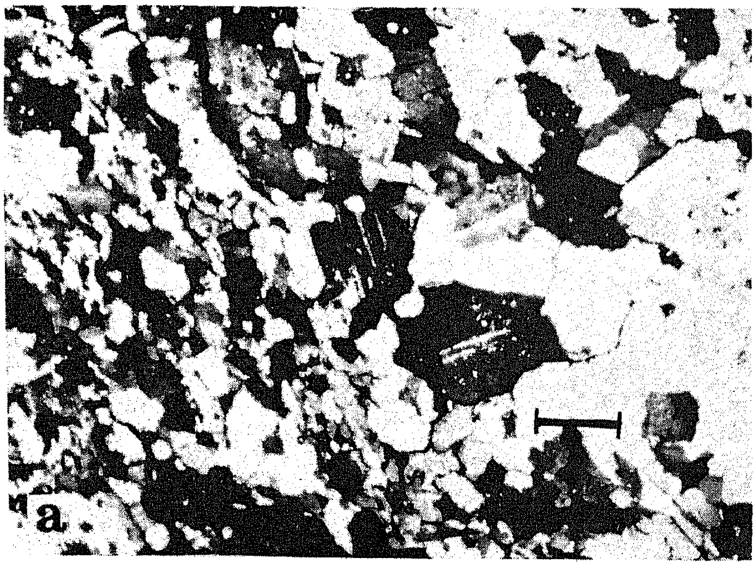

Figure 8(a). Mylonitic foliation defined by elongated quartz and plagioclase in the least-deformed variety of granite, undeformed part in the right hand side of the photograph, scale bar – 0·5 mm.

Figure 8(b). Type II S-C mylonite. Elongate quartz ribbons make an angle of 40° with C-plane, deformation band in one ribbon oblique to the elongation, scale bar – 0·2 mm.

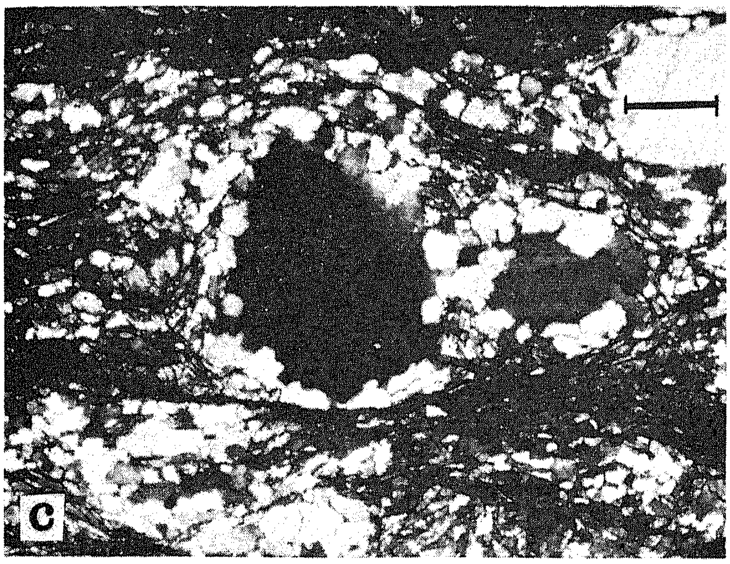

Figure 8(c). Core and mantle structure in quartz, scale bar – 0·2 mm.

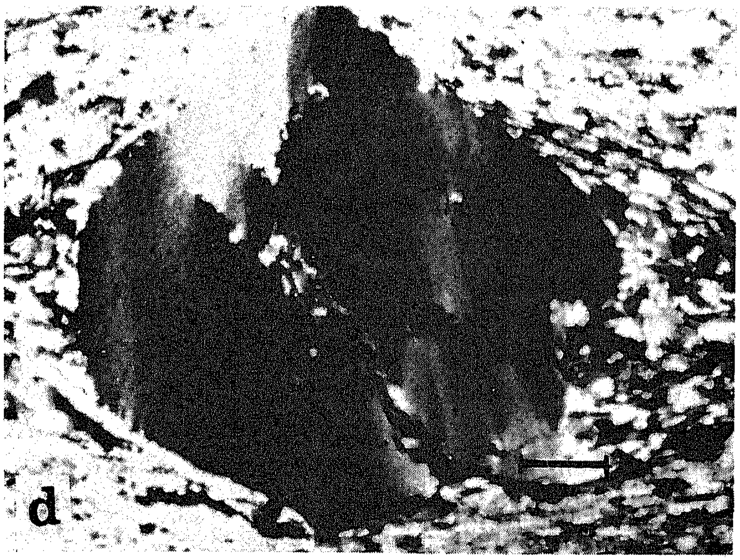

Figure 8(d). Highly-strained porphyroclast of quartz with deformation bands, shows recrystallization along linear zones, scale bar – 0·5 mm.

of recrystallization of quartz and polygonization of bent mica flakes. Rarely a cryptic banding defined by variation in grain size in quartzofeldspathic layers and associated tourmaline-rich layers is developed parallel to the axial planes of the folds.

Texturally the quartz-mica phyllonite resembles a type II S-C mylonite (Lister and Snoke 1984). The dominant micaceous foliation in the rock is marked by fine-grained and sheared-off mica flakes, concentration of opaques, and tiny recrystallized quartz grains. This represents the C-planes which have an anastomosing nature, and the elongate recrystallized quartz grains in the ribbons define the S-planes making an angle of 15°– 40° with the C-planes.

In the other rocks of the shear zone the megascopic schistosity, which acted as movement planes, represents a transposed foliation. Pre-existing oblique phyllosilicate

Table 1. Size of megacrysts of feldspar and of matrix grains in feldspathic schist, measured in sections perpendicular to foliation and parallel to lineation.

	Megacryst of feldspar			Matrix grains		
Slide no.	Range (mm)	Mean (mm)	Standard deviation	Range (mm)	Mean (mm)	Standard deviation
GD. 212	0·107–0·524	0·220(28)	0·081	0·016–0·059	0·032(117)	0·009
GD. 306	0·107–0·514	0·200(41)	0·080	0·016–0·061	0·032(108)	0·009
GD. 423	0·164–0·480	0·256(47)	0·071	0·010–0·063	0·031(115)	0·010
GD. 218	0·155–0·712	0·338(58)	0·126	0·013–0·042	0·025(104)	0·007
GD. 241	0·120–0·396	0·237(30)	0·067	0·008–0·037	0·019(106)	0·005
GD. 230	0·107–0·411	0·193(63)	0·066	0·009–0·028	0·018(110)	0·004
GD. 1104	0·120–0·208	0·152(11)	0·066	0·007–0·030	0·016(101)	0·005
GD. 1135	0·120–0·208	0·152(11)	0·033	0·007–0·030	0·016(106)	0·004

Numbers in brackets give the total number of grains measured.

laminae are rarely preserved and they show sigmoidal bending near the movement planes. Microstructural features in these rocks are similar to those observed in the granite mylonite and quartz-mica phyllonite.

4.2 *Deformation features in minerals*

Quartz: Grain size refinement caused by recrystallization is the commonly observed effect in quartz. The porphyroclasts display features of intracrystalline deformation (figure 8d), such as undulose extinction, planar deformation bands and development of equant or platy sub-grains. The site of recrystallization within the porphyroclasts varies from one grain to the other. At places recrystallization at margins of large grains has given rise to irregular, lobate or dentate boundaries, and has led to the development of 'core and mantle' structure (White 1976; figure 8c). Recrystallization may also start within a crystal along subgrain boundaries or deformation bands (figure 8d). Recrystallization has also taken place in the gaps separating the detached fragments of a porphyroclast. Deformation lamellae, where observed, are at high angles to the deformation bands; within a single crystal they show curvature while traversing from one deformation band to the next. In some rocks large grains of quartz are transformed into long ribbons showing planar deformation bands or elongate subgrains or grains with irregular to dentate margins. The deformation bands in the ribbons may be parallel or oblique to the elongation (figure 8b). In some of the more deformed mylonites flattened streaks made up of elongate recrystallized grains are observed. These represent quartz ribbons completely replaced by new grains. The fine recrystallized grains may have polygonal or elongate shape (figures 7a, 7c), the difference being explained as due to the difference in the rate of grain boundary migration relative to the imposed strain rate. If crystal plastic processes (intracrystalline slip) dominate the grains would tend to be elongated; on the contrary if grain boundary migration is relatively rapid the degree of elongation would be lower (Lister and Snoke 1984).

Feldspars: In comparison to quartz, feldspars exhibit more brittle behaviour. In the mylonites the porphyroclasts are of plagioclase (rarely microcline), which are broken

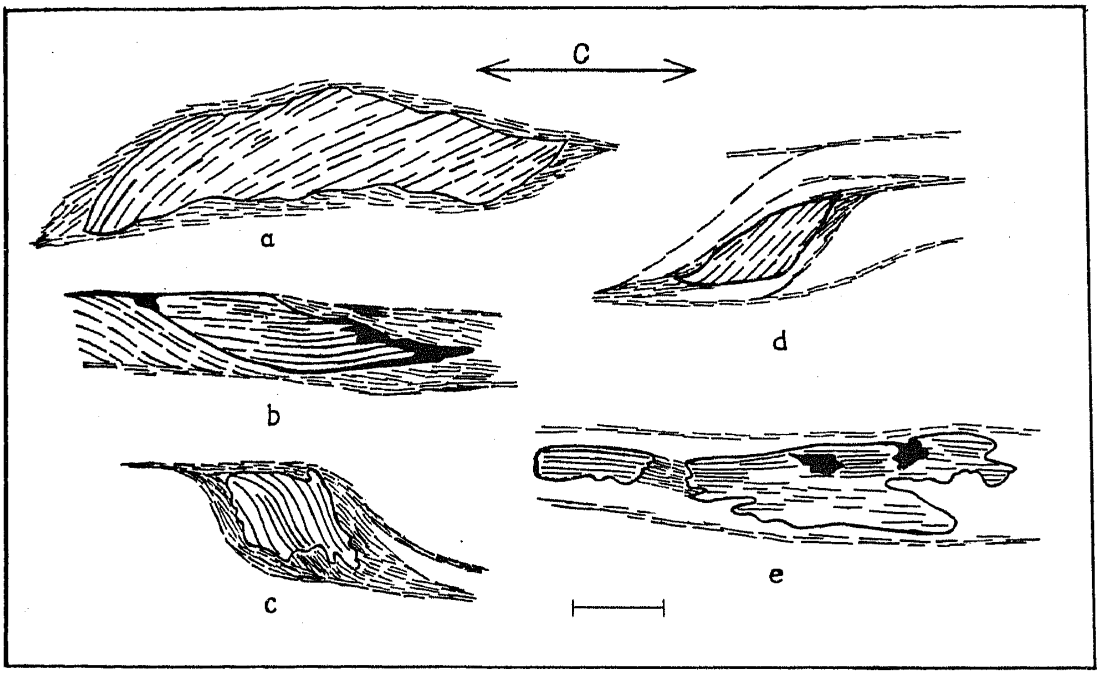

Figure 9. Sketch drawn from thin sections showing different relations of mica porphyroclasts to C-planes, scale bar – 0·2 mm.

into optically mismatched fragments with irregular boundaries. Sometimes rows of inclusions of quartz or sericite laminae cut across the porphyroclasts. Plagioclase typically shows tapering twin lamellae which are interpreted as secondary deformation twins (White 1975, 1976) and those die out towards the centre of the grains. The tapering twin lamellae may be bent and the axial planes of the bends are sometimes marked by fractures filled up with sericite. Grains with such bent and tapering twin lamellae show strong undulose extinction. Microfaulting of twin lamellae is also seen.

Muscovite: The flakes of muscovite defining the C-planes are often shredded and fine-grained. Large flakes are cut across at the edges by the straight C-planes (figures 9a, c, d), and sigmoidal bending of (001) planes gives rise to an oblique lenticular shape (mica 'fish'). The large flakes with (001) planes parallel or subparallel to the C-planes are usually pinched out at two ends to produce spindle shaped grains or are torn into lenticular boudins with tapering ends (figures 9b, e). Sometimes opaque minerals are concentrated at margins and along (001) planes of muscovite. Recrystallization has taken place at the edges of some large flakes of muscovite. In the zones separating the muscovite boudins greenish brown biotite has recrystallized.

5. Deformation mechanism

In the mylonites movement of dislocations is responsible for the ductile behaviour of quartz. The optical strain features including undulose extinction, planar deformation bands and subgrain formation with low angle boundaries, development of quartz ribbons subdivided into elongate subgrains or grains and the presence of strain features in the new recrystallized grains indicate that the dislocation creep type deformation was accompanied by dynamic recovery and dynamic recrystallization. This produced a steady flow in the rock (White 1977). The recrystallization process led to grain refinement. This reduction in grain size would probably cause a change in deformation mechanism from dislocation creep (power law creep) to grain size dependent creep (diffusional flow, superplasticity, Schmid 1982). Such a change in deformation mechanism would lead to strain softening.

Feldspars deformed in a more brittle fashion than quartz. However, the feldspars also record the features of intracrystalline deformation such as undulose extinction and mechanical twinning. The cleavage planes of feldspars may catalyse brittle deformation, and dislocation creep is probably impeded at the prevailing low temperature (chlorite-biotite zone) giving rise to the development of mechanical twinning (White 1975). Mechanical twinning in crystals result from partial dislocation and stacking faults (Hobbs *et al* 1976).

The ultramylonite bands in the feldspathic schists are suggestive of the onset of superplastic behaviour (Schmid 1982). The presence of two or more phases inhibits grain growth in such bands during deformation and recrystallization. Grain boundary sliding is thought to be the dominant mechanism in superplasticity (Boullier and Gueguen 1975). The phyllosilicates along the grain boundaries probably acted as effective lubricants during grain boundary sliding. The (001) planes of mica usually accommodate slip motion and consequently in a non-coaxial strain field (as indicated by the rotation of S-planes towards C-planes in the intensely deformed mylonites) the flakes of the phyllosilicate minerals undergo rotation towards parallelism with the flow planes giving rise to the mylonitic foliation (thin micaceous laminae which acted as movement planes). The mica flakes oblique to the movement direction either assume the typical spindle shape of mica 'fish' or get kinked depending upon the angular relation between the movement plane and the (001) planes of muscovite.

Fracturing of apatite and tourmaline needles point to their brittle deformation. Fracturing of the elongate grains probably has taken place by a fibre-loading mechanism (White *et al* 1980).

6. Indicators of shear sense

The following megascopic and microscopic structures have been utilized to deduce the sense of shear movement.

- The vergence of asymmetrical folds and crenulations on mylonitic foliation and banding. These are consistently sinistral on sections viewed from south or southeast.
- Acute angle relation between S- and C-planes (figure 6a), between C-planes and C′-planes (shear bands); sense of displacement on the C′-planes is also a useful indicator of shear sense (figure 3c).
- Sigmoidal shape of the oblique mica flakes (mica 'fish', figure 9) which are cut across at the edges by the movement planes.
- The acute angle between the elongate recrystallized grains of quartz in the quartz ribbons and the main foliation in the type II S-C mylonites (figure 8b).
- Asymmetric σ- and δ-type tails against porphyroclasts of feldspar, tourmaline or opaque-bearing knots (figure 7d). The porphyroclasts are rounded or elliptical in outline and in the latter case the elongation is generally oblique to the movement planes. It should be noted that σ- and δ-structures occur within the same thin section and this

suggests microscale variation in the intensity of deformation. As discussed by Passchier and Simpson (1986) σ-structure develops when the rate of recrystallization is high relative to the rate of rotation and the finite strain is low, whereas δ-structure develops when the rate of recrystallization is low and the finite strain is high. Asymmetric deflections of micaceous laminae around quartzofeldspathic porphyroclasts (figure 3d) resemble δ-structures and are also useful in determining the sense of shear.

The sense of shearing deduced from all these features confirms the bulk up-dip movement of overlying rocks along the Singhbhum shear zone.

7. Palaeostress estimation

It is generally considered that in dynamic recrystallization under steady state flow, the size of the recrystallized grains depends on flow stress, and the relationship is given by the following equation (White 1979):

$$\sigma = Kd^{-u}$$

σ = flow stress; d = grain diameter; K, u = constants.

Different estimates for the constants have been given by different workers (Twiss 1977; Mercier *et al* 1977; Ord and Christie 1984). For the present work only those samples of ultramylonites (fieldspathic schists) which show a uniform grain size in the quartzofeldspathic bands have been considered for palaeostress estimation. The mean grain size is calculated using the following formula:

$$D = 1/n \quad (D_{ia}D_{ib})^{1/2},$$

where D_{ia} and D_{ib} are the longest and shortest intercepts on each grain and n is the number of grains measured. The grain size data and the computed palaeostress estimates are given in table 2. Mercier's equation gives the lowest estimate of σ and the value computed according to the equation of Ord and Christie is greater than that according to Twiss (1977) by a factor of 2. The range of computed flow stress is similar

Table 2. Size of recrystallized quartz grains and palaeostress estimates. Flow stresses are calculated using equations:
I. Twiss (1977) $\sigma = 603\,(D)^{-0\cdot68}$; **II.** Mercier *et al* (1977) $\sigma = 381\,(D)^{-0\cdot71}$; **III.** Ord and Christie (1984) $\sigma = 4090\,(D)^{-1\cdot11}$; D is average grain diameter.

Specimen no.	Average diameter in mm (D)	Standard deviation	Palaeostress in MPa		
			I	II	III
GD. 212	0·032(117)	0·009	57·12	32·53	87·30
GD. 306	0·032(108)	0·009	57·12	32·53	87·30
GD. 423	0·031(115)	0·010	58·37	33·27	90·43
GD. 218	0·025(104)	0·007	67·56	38·76	114·82
GD. 241	0·019(106)	0·005	81·43	47·10	155·71
GD. 230	0·018(110)	0·004	84·48	48·94	165·34
GD. 1104	0·016(101)	0·005	91·52	53·21	188·43
GD. 1135	0·016(106)	0·004	91·52	53·21	188·43

Numbers in brackets give the total number of grains measured.

to that obtained for the Moine thrust in Scotland (50–130 MPa; Twiss 1977; White 1979). However, uncertainties exist in estimating the flow stress from the grain size, because the latter is influenced by the presence of other phases like mica and chlorite, the chemical environment during deformation, e.g. presence of water, annealing recovery or recrystallization, etc.

8. Structural evolution

The deformation features developed in the minerals and the mylonitic fabric of the rocks confirm that the Singhbhum shear zone is a ductile deformation zone in which the structurally higher (northern) horizons had an up-dip movement.

Mylonitization within the shear zone represents an early deformational episode. Where the mylonitic fabric is not developed, the schistosity axial planar to the early reclined folds on compositional banding represents the earliest formed secondary planar structure; its orientation is parallel to the mylonitic foliation. The consistent down-dip stretching lineation developed on the mylonitic foliation and on the axial planar schistosity represents the direction of maximum elongation.

The generation of successive sets of mylonitic foliation, folding of the earlier sets and their truncation by the later ones, resulted from progressive shearing movement. Although locally superposition relationships can be seen, the isoclinal reclined folds and the sinistral folds with gently plunging axes and steep dipping axial planes possibly represent the earlier and later stages of this progressive deformation. The geometric variations shown by the sinistral folds are due to their development at different stages of deformation and variable rotation of their axial planes and axes towards the shear planes and shear direction respectively. The main mylonitic foliation represents coplanar S- and C-planes, the two being brought into parallelism by the intensity of deformation. Oblique S- and C-planes possibly record the strain during the waning stage of movement. The shear bands were developed at the very last stage and caused sigmoidal curvature of the earlier foliations. The transverse warps belong to a distinctly later episode of longitudinal compression. The mylonitic foliation within the shear zone is parallel to the schistosity outside it, and reclined folds of identical orientation are present inside and outside the shear zone. This leads us to conclude that the mylonitization was broadly coeval with the early deformation episode within the North Singhbhum fold belt.

Acknowledgements

The work was carried out at the Department of Applied Geology, Indian School of Mines, Dhanbad, and was partly funded by the DST under the Thrust Area Programme. We are grateful to Hindustan Copper Limited for providing complete facilities for our field work at Mosabani.

References

Berthe D, Choukroune P and Jegouzo P 1979 Orthogneiss. mylonite and non-coaxial deformation of granites: The example of the south Armorican shear zone; *J. Struct. Geol.* **1** 31–42

Boullier A M and Gueguen Y 1975 SP mylonites:Origin of some mylonites by superplastic flow; *Contrib. Mineral. Petrol.* **50** 93–104

Cobbold P R and Quinquis H 1980 Development of sheath folds in shear regimes; *J. Struct. Geol.* **2** 119–126

Dasgupta S, Deb G, Mukhopadhyay D, Chadwick B, Sengupta S and Van Den Hul H J 1993 A study of acid magmatism in eastern part of the Singhbhum shear zone, Bihar India; *Proc. Natl. Acad. Sci. India,* **A63** 223–251

Deb G and Mukhopadhyay D 1991 An occurrence of tourmalinite along Singhbhum shear zone; *Indian Minerals* **45** 313–318

Dunn J A and Dey A K 1942 The geology and petrology of eastern Singhbhum and surrounding areas; *Mem. Geol. Surv. India* **69** 1–456

Ghosh S K and Sengupta S 1987 Progressive development of structures in a ductile shear zone; *J. Struct. Geol.* **9** 277–287.

Ghosh S K and Sengupta S 1990 Singhbhum shear zone: Structural transition and a kinematic model; *Proc. Indian Acad. Sci.* (*Earth Planet. Sci.*) **99** 229–247

Gray D R 1977 Morphological classification of crenulation cleavage; *J. Geol.* **85** 229–235

Hobbs B E, Means W D and Williams P F 1976 *An outline of structural geology.* (New York: John Wiley) 571 p

Lister G S and Snoke A W 1984 S-C mylonites; *J. Struct. Geol.* **6** 617–638

Mercier J C, Anderson D A and Carter N L 1977 Stress in the lithosphere. Inferences from steady state flow of rocks; *Pure Appl. Geophys.* **115** 119–226

Mukhopadhyay D, Ghosh A K and Bhattacharya S 1975 A reassessment of the structures in the Singhbhum shear zone; *Bull. Geol. Min. Metall. Soc. India* **48** 49–67

Naha K 1965 Metamorphism in relation to stratigraphy, structure and movements in part of east Singhbhum, eastern India *Q. J. Geol. Min. Metall. Soc. India* **37** 41–85

Ord A and Christie J M 1984 Flow stresses from microstructures in mylonitic quartzites from the Moine thrust zone, Assynt area, Scotland; *J. Struct. Geol.* **6** 639–654

Passchier C W and Simpson C 1986 Porphyroclast system as kinematic indicators; *J. Struct. Geol.* **8** 831–843

Platt J P 1979 Extensional crenulation cleavage; *J. Struct. Geol.* **1** 95

Platt J P and Vissers R L M 1980 Extensional structures in anisotropic rocks; *J. Struct. Geol.* **2** 397–410

Sarkar S N and Saha A K 1962 A revision of the Precambrian stratigraphy and tectonics of Singhbhum and adjacent regions; *Q. J. Geol. Min. Metall. Soc. India* **34** 97–136

Schmid S M 1982 Microfabric studies as indicators of deformation mechanisms and flow laws operative in mountain building. In *Mountain building processes: An introduction* (ed) K J Hsu, (London: Academic Press) 95–110

Simpson C 1984 Borrego Springs-Santa Rosa mylonite zone: A late Cretaceous west-directed thrust in southern California; *Geology* **12** 8–11

Simpson C and Schmid S M 1983 An evaluation of criteria to deduce the sense of movement in sheared rocks; *Bull. Geol. Soc. Am.* **94** 1281--1288

Twiss R J 1977 Theory and applicability of a recrystallized grain size palaeopiezometer; *Pure Appl. Geophys.* **115** 227–244

White S 1975 Tectonic deformation and recrystallization of oligoclase; *Contrib. Mineral. Petrol.* **50** 287–305

White S 1976 The effects of strain on the microstructures, fabrics and deformation mechanisms in quartzites; *Philos. Trans R. Soc. London* **A283** 69–86

White S 1977 Geological significance of recovery and recrystallization processes in quartz; *Tectonophysics,* **39** 143–170

White S, 1979: Grain and sub-grain size variations across a mylonite zone; *Contrib. Mineral. Petrol.* **70** 193–202

White S H, Burrows S E, Carreras J, Shaw N D and Humphreys F J 1980 On mylonites in ductile shear zones; *J. Struct. Geol.* **2** 175–187